

Available online at www.sciencedirect.com

jmr&t
Journal of Materials Research and Technology
journal homepage: www.elsevier.com/locate/jmrt



Original Article

Microstructure evolution of additively manufactured CoCrFeNiAl_{0.4} high-entropy alloy under thermo-mechanical processing



Qiang Li ^a, Xiao Chen ^b, Xizhang Chen ^{a,e,*}, Arshad Noor Siddiquee ^c, Vladislav B. Deev ^d, Sergey Kononov ^e, Ming Wen ^f

^a School of Mechanical and Electrical Engineering, Wenzhou University, Wenzhou, 325035, Zhejiang, China

^b School of Materials Science and Engineering, China University of Petroleum (East China), Qingdao, Shandong, 266580, China

^c Department of Mechanical Engineering, Jamia Millia Islamia, New Delhi, India

^d Department of Metal Forming of National University of Science and Technology, "MISIS", Russia

^e Department of Metals Technology and Aviation Materials, Samara National Research University, 34, Moskovskoye Shosse, Samara, 443086, Russia

^f Yunnan Key Lab of Precious Metallic Materials, Kunming Institute of Precious Metals, Kunming, Yunnan, 650106, China

ARTICLE INFO

Article history:

Received 4 October 2021

Accepted 2 December 2021

Available online 6 December 2021

Keywords:

Thermo-mechanical processing

Powder plasma arc additive manufacturing

Work hardening rate

Texture evolution

Recrystallization

ABSTRACT

The microstructure and texture evolution during thermo-mechanical processing (TMP) and their relationship with the mechanical properties in the non-equiatomic CoCrFeNiAl_{0.4} high-entropy alloy (HEA) were investigated. In this work, a combination of cold rolling and annealing technology was used to investigate the HEA which has been fabricated by powder plasma arc additive manufacturing (PPA-AM) in the deformed and recrystallized states. Microstructure and texture analysis were performed by electron backscatter diffraction. The mechanical properties were evaluated using static tensile testing. It was substantiated that annealing twins facilitates the transition from the cube texture to the shear texture and has a great influence on the evolution of texture after TMP. Based on the research of CoCrFeNiAl_{0.4} high-entropy alloy, thermo-mechanical processing under appropriate conditions can increase the work hardening rate, but the work hardening rate is relatively stable under 30%–45% plastic deformation. The correlation during TMP between mechanical properties and work hardening, texture evolution, and recrystallization was discussed.

© 2021 The Authors. Published by Elsevier B.V. This is an open access article under the CC BY-NC-ND license (<http://creativecommons.org/licenses/by-nc-nd/4.0/>).

1. Introduction

The high entropy alloys (HEAs) are regarded as materials of future which comprise of 5 or more elements with atomic

ratio of each is between 5% and 35%. The high-entropy effect of the HEAs makes it easier for the multi-component alloy to form a single-phase solid solution, and the sluggish diffusion effect makes the phase of multi-component alloys relatively stable even at high temperature [1]. The lattice-distortions

* Corresponding author.

E-mail addresses: Kernel.chen@gmail.com, chenxizhang@wzu.edu.cn (X. Chen).

<https://doi.org/10.1016/j.jmrt.2021.12.007>

2238-7854/© 2021 The Authors. Published by Elsevier B.V. This is an open access article under the CC BY-NC-ND license (<http://creativecommons.org/licenses/by-nc-nd/4.0/>).

and the cocktail effect make it possible for the high entropy alloy to have many sought-after mechanical properties, such as the high yield strength [2], better corrosion resistance [3,4], high strength and hardness [5,6], and good thermal stability [7,8], etc. Ever since the HEAs was defined and named by Yeh and Cantor et al. [9,10], it has gained a lot of attention from researchers around the world.

Commonly, the high value of configurational entropy makes it easier for HEAs to form disordered solid solutions such as Face-Centered-Cubic (FCC), Body-Centered-Cubic (BCC), and Hexagonal- Close-Packed (HCP), rather than forming intermetallic compounds (IMCs). The single-phase solid solution HEAs inherit characteristics of their basic structure in terms of dominance in properties associated with the structure. The FCC-HEAs exhibit a good ductility but a lower yield strength due to their FCC structural characteristics [11,12]. The structure of HEAs bears a great significance during the post fabrication thermo-mechanical processing (TMP) [13]. The structure evolution in FCC-HEAs after TMP induce plastic deformation significantly influences the mechanical properties of HEAs. In addition, whether it is the texture evolution of the FCC-HEAs or its plastic deformation mechanism, they all depend greatly on the stacking fault energy (SFE) [14–17]. FCC-HEAs have been long sought for their many desirable mechanical attributes [18]. Gludovatz et al. [19] reduced the temperature to transform the plane slip dislocation at room temperature into deformation twins to obtain CoCrFeNiMn FCC-based alloy with excellent mechanical properties. The CoCrNi FCC-based alloy induces twinning by plastic deformation, resulting in an increase in strength and ductility [20]. More and more scientific activities have focused on systematic research on the FCC-HEAs to improve mechanical properties and reveal deformation mechanism [18,21,22].

To promote the mechanical properties of HEAs as structural materials, it is highly desirable to improve the strength of HEAs while maintaining good ductility. The traditional way of designing and controlling the microstructure is to carry out appropriate alloying and heat treatment of the material [23]. The TMP treatment combining the plastic deformation with heat treatment such as water quenching, heating, and cooling at different rates can attain tailored microstructure and resultant mechanical properties [24]. Compared with hot

rolling, cold rolling can attain relatively fine grains and reduce the recrystallization temperature of the alloy [25], leading to significant reduction in energy required for recrystallization. However, underlying deformation mechanism during TMP of HEAs is very scantily reported.

The routes of preparing HEAs include vacuum arc casting [26,27], laser cladding [28], plasma sintering [29], wire-arc additive manufacturing [30,31] and powder metallurgy [32], etc. However, these routes have a number limitation with regard to single preparation shape, high cost, and low manufacturing efficiency, which limit the wide application of this technology [33,34]. The powder plasma arc additive manufacturing technology used in this paper can overcome these shortcomings and produce finer grain HEAs.

In this work, the CoCrFeNiAl_{0.4} HEA was prepared by powder plasma arc additive manufacturing technology, followed by TMP. The TMP was performed to induce various degree of cold-work via rolling to study the plastic deformation mechanism. In order to demonstrate the plastic deformation mechanism in the developed HEAs, (i) Work hardening behavior of FCC CoCrFeNiAl_{0.4} HEA during TMP, (ii) Effect of TMP with different degrees of cold rolling of texture evolution and (iii) Recrystallization behavior of HEAs under different plastic deformations was performed.

2. Materials and methods

The purity of the elemental metal powder used in this study is greater than 99.5%, and the powder particle size is 150–325 mesh. The mixed elemental powder and alumina grinding balls are effectively mechanically alloyed in a high-energy planetary ball mill filled under protective gas at a volume ratio of 1:1.5 for 6 h to make powder homogenization. The powder plasma arc additive manufacturing equipment was used to deposit layer by layer. During the deposition process, an angle grinder was used to remove the metal oxide layer on the surface of the deposited layer. CoCrFeNiAl_{0.4} HEA block was prepared with a wire-cut electric discharge machine to prepare cold-rolled specimens. The processing diagram and scheme of sampling location are shown in Fig. 1.

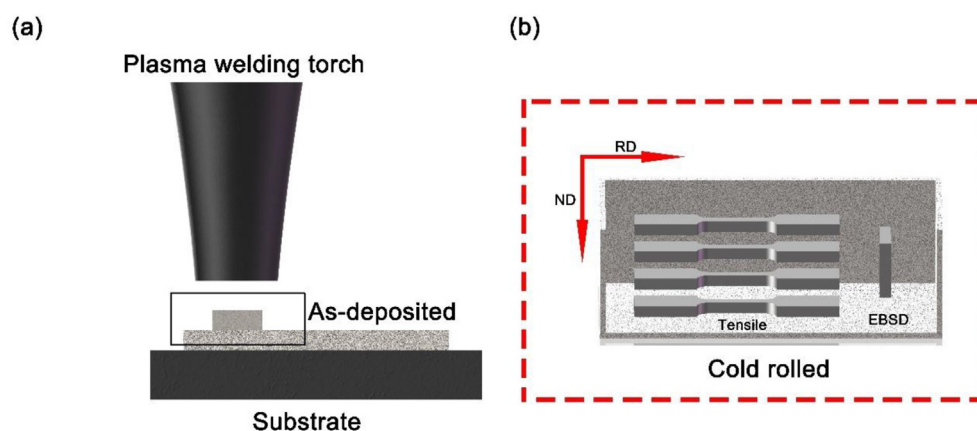


Fig. 1 – (a) Schematic diagram of high-entropy alloys fabricated by powder plasma arc additive manufacturing (PPA-AM) and (b) schematic showing the location of samples taken for microstructural evaluation.

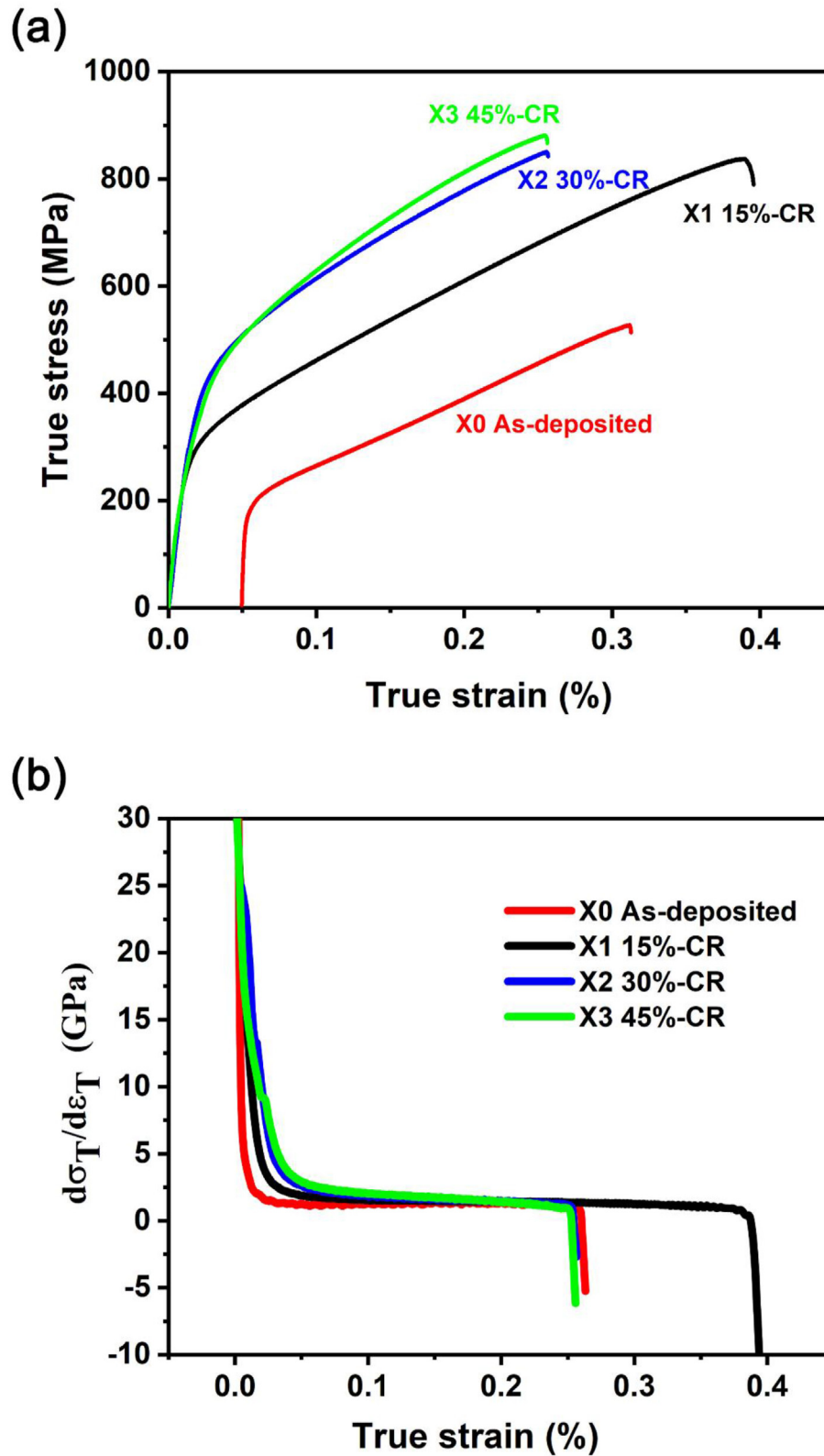


Fig. 2 – (a) True stress–strain and (b) Work-hardening rate–true strain curve of $\text{CoCrFeNiAl}_{0.4}$ under different plastic deformation.

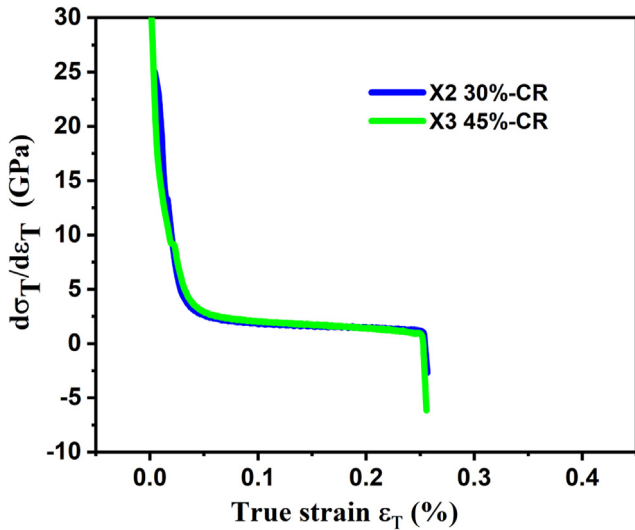


Fig. 3 – Work-hardening rate-true strain curve of CoCrFeNiAl_{0.4} under 30% and 45% plastic deformation.

The dog-bone shaped specimens were used for the tensile tests and tensile test was conducted using the universal testing machine (E45.105) at room temperature with a strain rate of 10^{-3}s^{-1} . The texture evolution and recrystallization behavior were investigated by electron backscatter diffraction (EBSD, Oxford Nordly Max3, Oxford Instrument Technology Co., Ltd.).

3. Result & discussion

In this paper, CoCrFeNiAl_{0.4} HEA was prepared by powder plasma arc additive manufacturing technology, and then cold

rolled to reduce the thickness of alloys by 15%, 30% and 45%. The as-prepared samples were kept at 1000 °C for 1 h followed by water quenching. X0, X1, X2, and X3 represent the as-deposited sample and the samples with 15%, 30%, and 45% cold-rolled deformation, respectively.

3.1. Behavior of work hardening

The cold-work significantly enhances the dislocation density causing increase in strength of the alloys under conditions of plastic deformation. The mechanical properties of CoCrFeNiAl_{0.4} HEA under different extent of plastic deformations were measured by tensile tests at room temperature (Fig. 2a).

The yield strength (YS) and the ultimate tensile strength (UTS) of the as-deposited HEA are 253 MPa and 527 MPa, respectively, as shown in Fig. 2a. Both YS and UTS increased after the TMP. Accordingly, the YS and UTS increased by ~110% and ~67% to ~530 MPa and ~880 MPa, respectively. In addition, the fracture strain of sample X1 HEA is found to be ~38.9%, which is an increase of 24.7%. For sample X1, YS and UTS are measured at ~360 MPa and ~837 MPa, respectively. It is evident that the sample X2 has better UTS than the X1. The enhancement in the strength of sample X2 HEA is attributed to twinning in the deformation process and provides additional work hardening [35]. Work hardening plot of CoCrFeNiAl_{0.4} HEA is shown in Fig. 2b. The interaction of dislocations and twins leads to HEA with good mechanical properties and high work hardening ability [36,37].

The twins offer obstacle to the dislocation slip and increase dislocation density through pileup [38]. But, the work hardening rate at room temperature continues to decrease as the strain increases, because the twins are not activated until the fracture [35].

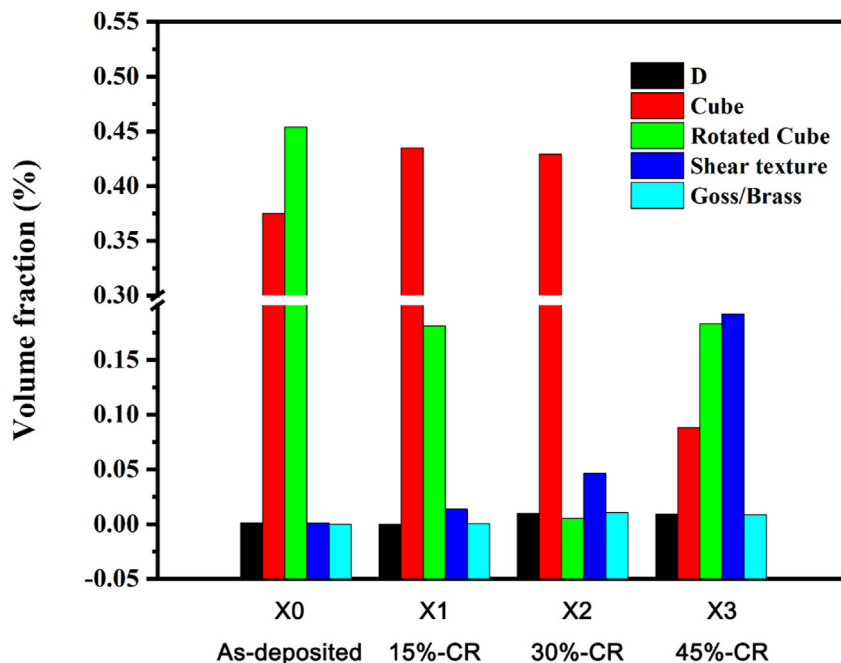


Fig. 4 – Volume fraction of texture component of the CoCrFeNiAl_{0.4} HEA subjected to thermo-mechanical processing.

Table 1 – Texture component in the CoCrFeNiAl_{0.4} HEA under different extent plastic deformations.

Texture component	Miller indices	φ_1	Φ	φ_2	Symbol
D	{113} <332>	90	27	45	1
Cube	{001} <100>	0	0	0	2
Rotated cube	{100} <011>	0	0	45	3
Shear texture	{112} <110>	0	35	45	4
Goss/Brass	{110} <111>	55	45	0	5

The work-hardening-rate to true-strain curve of the CoCrFeNiAl_{0.4} HEA (Fig. 2b), shows that, except for the as-deposited alloy, all TMP treated samples have two inflection points. Compared with the as-deposited X0 whose work hardening rate decreases monotonously, the work hardening rate of the thermo-mechanical processing samples follow the trend of first decrease, and then increase. With the increasing of cold rolling deformation, it provides the energy for dislocation nucleation inside the recrystallized grains. Therefore, the work hardening rate of the thermomechanical treated specimens first decreases and then increases [39]. The work hardening rate curve of X0 is similar to the high SFE alloys, while X1, X2 and X3 with two inflection subdivided into 5 states by Gutierrez et al. [40,41]. The first inflection point is usually related to the formation of dislocation substructures composed of dislocation unit cells and high-density dislocation shear bands [42]. The work hardening rate of the CoCrFeNiAl_{0.4} HEA is improved by thermo-mechanical

treatment. However, X2 and X3 have almost the same work hardening rate, the curves of X2 and X3 nearly coincide (Fig. 3). It can be inferred that the work hardening rate does not increase indefinitely with the increase in the amount of cold rolling deformation.

3.2. Texture evolution

The volume fraction of texture during TMP are shown by ODF sections (Fig. 6) and quantitative analysis the volume fractions of rolling texture components (Fig. 4).

Above a different extent plastic deformation, in the ODF sections characteristic texture components of CoCrFeNiAl_{0.4} HEA are seen, like D, cube, rotated cube, etc (for definition see Table 1). The main texture components in the HEA for different amount of cold rolling plastic deformation are very similar to the one's belonging to the as-deposited sample, and the texture mainly composed of cube texture ({001} <100>), rotated cube texture ({100} <011>) and shear texture ({112} <110>). The D texture component disappear compared to the as-deposited sample, which shows a maximum intensity of ~1.9. With the increase in the amount of cold rolling plastic deformation, the strength of rotated cube texture and shear texture are greatly increased, and the maximum intensity of the two textures is ~9.4 and ~13, respectively, accompanied by the decrease of cube texture ({001} <100>). An increase in the thickness reduction to 45%, the development of Goss/Brass texture ({110} <111>) as a new component can be observed in the $\varphi_2 = 85^\circ$ section of

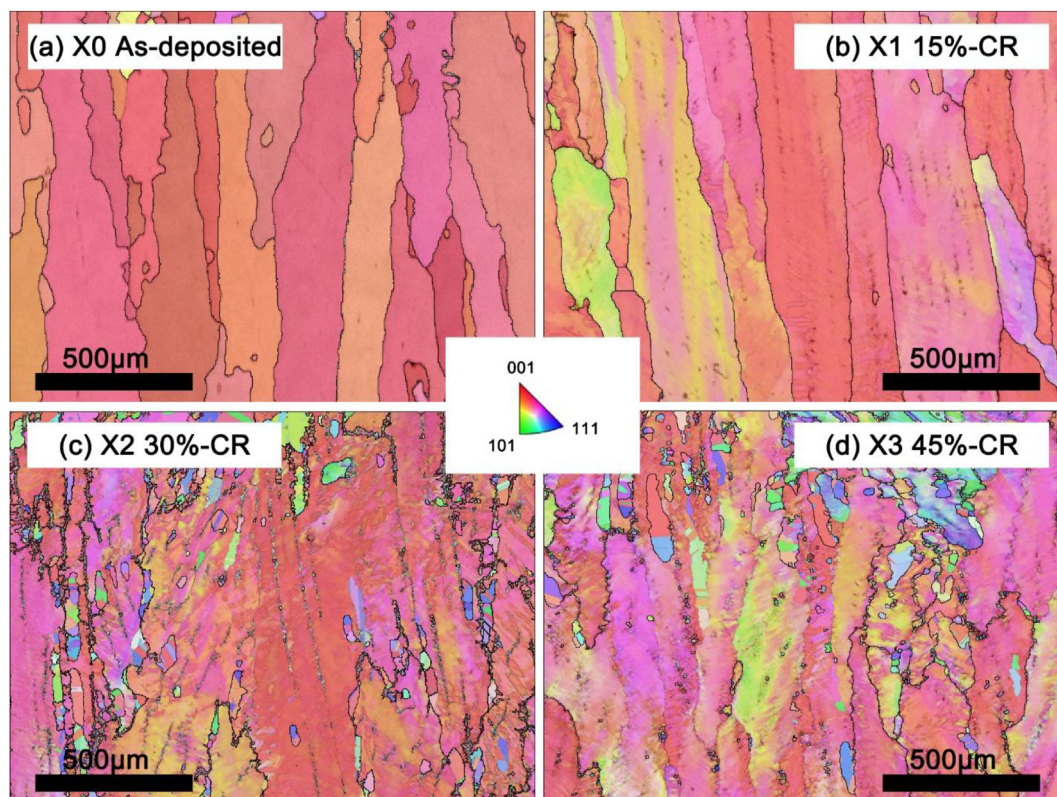


Fig. 5 – IPF of CoCrFeNiAl_{0.4} HEA (a) X0 as-deposited, (b) X1 15%-CR, (c) X2 30%-CR and (d) X3 45%-CR.

ODFs of the $\text{CoCrFeNiAl}_{0.4}$. However, the rotated cube texture with the intensity of 1.9 remains relative stable. In addition, shear texture with the intensity of 11 can be seen in the $\phi_2 = 45^\circ$ section of the ODF for the 45% cold-rolled sample. It is worth noting that the volume fraction of shear texture increases sharply after the cold rolling deformation indicating that the strength of the shear texture is affected by the plastic deformation, as has been reported in the previous literature [43].

Annealing twins appeared in the IPF maps (Fig. 5) of $\text{CoCrFeNiAl}_{0.4}$ HEA leading to sharply increase in shear texture and cubic texture when the reduction of thickness reaches to 30% during TMP. The main reason for this texture evolution may be the appearance of annealing twins [44]. It can be seen from the statistical volume fraction diagram of typical texture (Fig. 4) that $\text{CoCrFeNiAl}_{0.4}$ HEA produced by powder plasma arc additive manufacturing (PPA-AM) weakens the preferred

orientation of the initial texture and increases the volume fraction of the random texture under the condition of small plastic deformation. Thermo-mechanical treatment with a larger amount of deformation may further change the preferred orientation of the overall texture.

3.3. Behavior of recrystallization

Commonly, recrystallization is usually used to describe the phenomenon that the deformed structure is replaced by new grains during the annealing process [45]. The energy for new grain growth is stored by dislocations and sub-boundaries during plastic deformation. During TMP, the dislocation density is increased due to cold rolling plastic deformation, which supplies initial energy for the recrystallization of the alloys.

The recrystallization map (Fig. 7) consists of red, blue and yellow parts, which represent deformed structure,

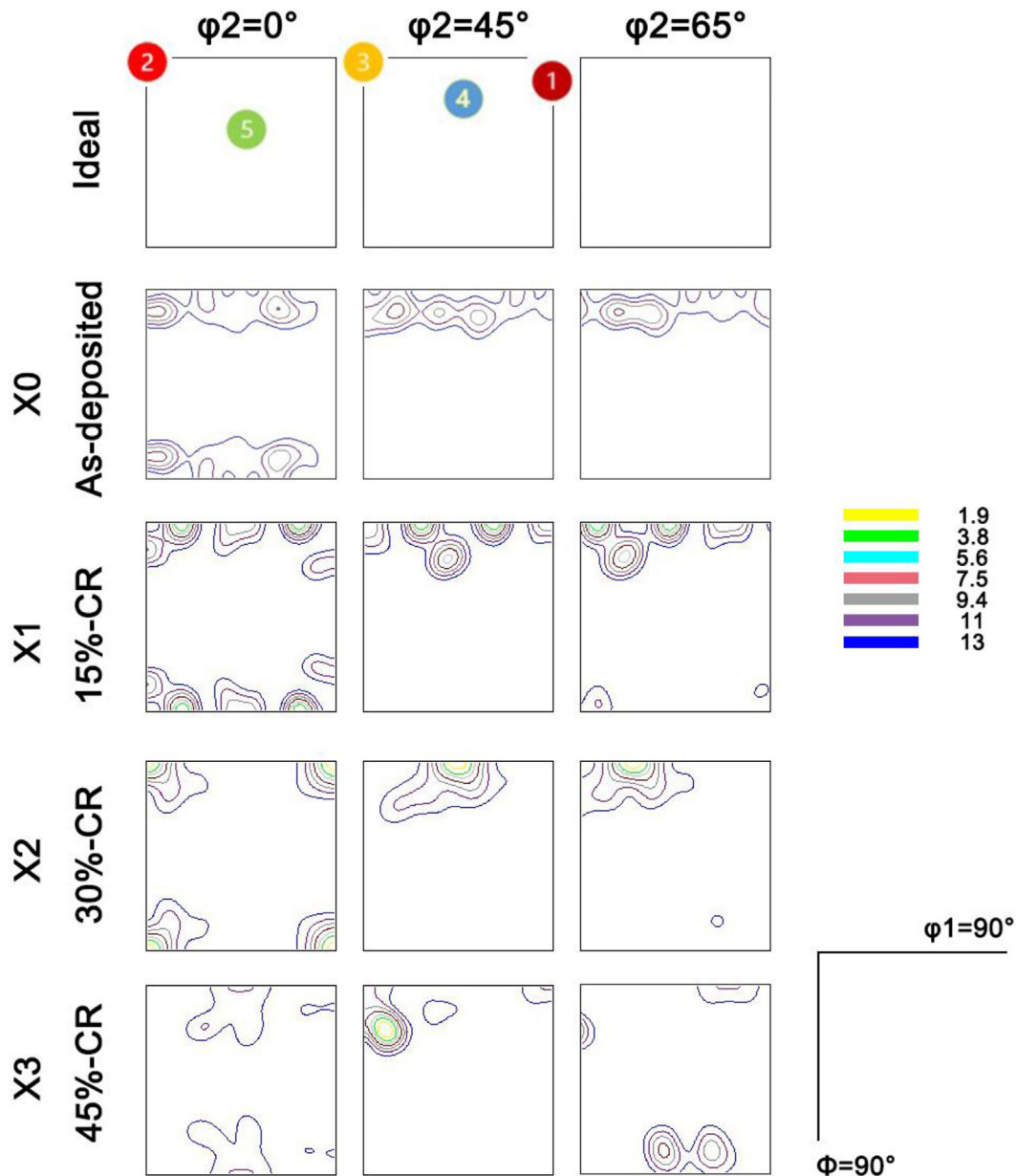


Fig. 6 – The $\phi_2 = 0^\circ, 45^\circ$ and 65° sections of the ODFs of the $\text{CoCrFeNiAl}_{0.4}$ during thermo-mechanical processing.

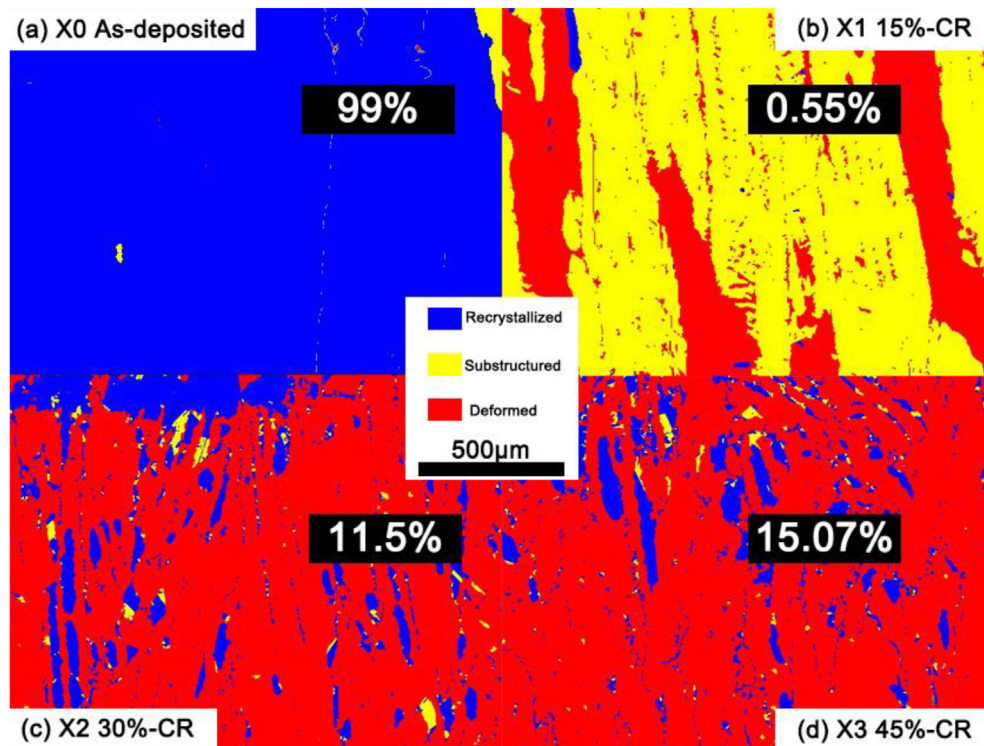


Fig. 7 – DefRex map of CoCrFeNiAl_{0.4} HEA (a) X0 As-deposited, (b) X1 15%-CR, (c) X2 30%-CR and (d) X3 45%-CR.

recrystallized structure and substructures, respectively. The red deformed structure is full of dislocations, the yellow other structures can absorb dislocations, and the blue recrystallized structure has almost no dislocations [46]. During the thermo-mechanical treatment of HEA, the volume fraction of recrystallized grains keeps increasing with the amount of cold rolling plastic deformation. Meanwhile, twins are mainly concentrated in the non-recrystallized grains under the 30% plastic deformation, while there are almost no twins in the recrystallized grains. This phenomenon is attributed to the fact that recrystallized grains containing a small amount of dislocations cannot induce deform twinning, so in the recrystallized grains is annealing twins [47]. It can be seen from the recrystallization map that the structure has not undergone TMP is almost completely recrystallized, while samples having higher degree of cold rolling plastic deformation showed increasing rate of recrystallization. This indicates that the recrystallization of CoCrFeNiAl_{0.4} HEA starts at a small amount of plastic deformation, causing a large numbers of dislocations to provide energy for recrystallization [48]. The recrystallized grains have the characteristics of low strength and high plastic deformation ability [47], thermo-mechanical processing is used to adjust the recrystallization degree of alloy, and simultaneously improve the strength and ductility.

4. Conclusions

In this study, an innovative plasma arc additive manufacturing technology was used to fabricate non-equiatom CoCrFeNiAl_{0.4} HEA, which has been subject to

thermo-mechanical processing. The effect of cold rolling followed by annealing on its work hardening ability, texture evolution and recrystallization behavior was studied. The following are the conclusions:

1. Thermo-mechanical processing can improve the work hardening rate of CoCrFeNiAl_{0.4} HEA, but the work hardening rate will not increase continuously with the increase of plastic deformation. In this paper, the work hardening rate of CoCrFeNiAl_{0.4} HEA becomes relatively stable after thickness reduction more than 30% due to annealing twins.
2. The texture evolution of CoCrFeNiAl_{0.4} HEA during thermo-mechanical processing is closely related to annealing twins.
3. Thermo-mechanical processing with a small deformation can weaken the intensity of the initial texture and increase the volume fraction of random texture.
4. Tailoring the volume fraction of deformed grains filled with dislocations and recrystallized grains with higher ductility can overcome the trade-off of strength and toughness.

Declaration of Competing Interest

The authors declare that they have no known competing financial interests or personal relationships that could have appeared to influence the work reported in this paper.

Acknowledgements

This work is supported by National Natural Science Foundation of China (Grant No. 51975419).

REFERENCES

- [1] Zou Y, Wheeler JM, Ma H, Okle P, Spolenak R. Nanocrystalline high-entropy alloys: a new paradigm in high-temperature strength and stability. *Nano Lett* 2017;17:1569–74. <https://doi.org/10.1021/acs.nanolett.6b04716>.
- [2] Senkov ON, Wilks GB, Scott JM, Miracle DB. Mechanical properties of Nb₂₅Mo₂₅Ta₂₅W₂₅ and V₂₀Nb₂₀Mo₂₀Ta₂₀W₂₀ refractory high entropy alloys. *Intermetallics* 2011;19:698–706. <https://doi.org/10.1016/j.intermet.2011.01.004>.
- [3] Tang S, Dai Z, Tan G, Gong S, Liu B, Xie G, et al. High-strength, ductility and corrosion-resistant in a novel Cu₂₀Ni₂₀Mn_{0.3}Cr_{0.3}Al alloy. *Mater Chem Phys* 2020;252:123177. <https://doi.org/10.1016/j.matchemphys.2020.123177>.
- [4] Liu B, Liu J, Liu Y, Gong S, Dai Y, Zhao G, et al. Effects of Al addition on corrosion behavior and mechanical property of high-strength and high-elasticity Cu-20Ni-20Mn-0.3Nb-0.3Cr-0.3Zr alloy. *Mater Char* 2020;167:110476. <https://doi.org/10.1016/j.matchar.2020.110476>.
- [5] Ma SG, Zhang Y. Effect of Nb addition on the microstructure and properties of AlCoCrFeNi high-entropy alloy. *Mater Sci Eng, A* 2012;532:480–6. <https://doi.org/10.1016/j.msea.2011.10.110>.
- [6] Zhou YJ, Zhang Y, Wang YL, Chen GL. Solid solution alloys of AlCoCrFeNiTi_x with excellent room-temperature mechanical properties. *Appl Phys Lett* 2007;90:181904. <https://doi.org/10.1063/1.2734517>.
- [7] Huang P-K, Yeh J-W. Inhibition of grain coarsening up to 1000°C in (AlCrNbSiTiV)_N superhard coatings. *Scripta Mater* 2010;62:105–8. <https://doi.org/10.1016/j.scriptamat.2009.09.015>.
- [8] Singh S, Wanderka N, Murty BS, Glatzel U, Banhart J. Decomposition in multi-component AlCoCrCuFeNi high-entropy alloy. *Acta Mater* 2011;59:182–90. <https://doi.org/10.1016/j.actamat.2010.09.023>.
- [9] Cantor B, Chang ITH, Knight P, Vincent AJB. Microstructural development in equiatomic multicomponent alloys. *Mater Sci Eng, A* 2004;375–377:213–8. <https://doi.org/10.1016/j.msea.2003.10.257>.
- [10] Yeh J-W. Recent progress in high-entropy alloys. *Eur J Control - EUR J CONTROL* 2006;31:633–48. <https://doi.org/10.3166/acsm.31.633-648>.
- [11] Wu SW, Wang G, Yi J, Jia YD, Hussain I, Zhai QJ, et al. Strong grain-size effect on deformation twinning of an Al_{0.1}CoCrFeNi high-entropy alloy. *Mater Res Lett* 2017;5:276–83. <https://doi.org/10.1080/21663831.2016.1257514>.
- [12] Sun SJ, Tian YZ, Lin HR, Dong XG, Wang YH, Zhang ZJ, et al. Enhanced strength and ductility of bulk CoCrFeMnNi high entropy alloy having fully recrystallized ultrafine-grained structure. *Mater Des* 2017;133:122–7. <https://doi.org/10.1016/j.matdes.2017.07.054>.
- [13] Hou J, Qiao J, Lian J, Liaw PK. Revealing the relationship between microstructures, textures, and mechanical behaviors of cold-rolled Al_{0.1}CoCrFeNi high-entropy alloys. *Mater Sci Eng - Struct Mater Prop Microstruct Process* 2021;804:140752. <https://doi.org/10.1016/j.msea.2021.140752>.
- [14] Bhattacharjee PP, Sathiaraj GD, Zaid M, Gatti JR, Lee C, Tsai C-W, et al. Microstructure and texture evolution during annealing of equiatomic CoCrFeMnNi high-entropy alloy. *J Alloys Compd* 2014;587:544–52. <https://doi.org/10.1016/j.jallcom.2013.10.237>.
- [15] Sathiaraj GD, Kalsar R, Suwas S, Skrotzki W. Effect of stacking fault energy on microstructure and texture evolution during the rolling of non-equiatomic CrMnFeCoNi high-entropy alloys. *Crystals* 2020;10:607. <https://doi.org/10.3390/cryst10070607>.
- [16] Yan J, Fang W, Huang J, Zhang J, Chang R, Zhang X, et al. Plastic deformation mechanism of CoCr_xNi medium entropy alloys. *Mater Sci Eng, A* 2021;814:141181. <https://doi.org/10.1016/j.msea.2021.141181>.
- [17] El-Danaf E, Kalidindi SR, Doherty RD. Influence of grain size and stacking-fault energy on deformation twinning in fcc metals. *Metall Mater Trans A* 1999;30:1223–33. <https://doi.org/10.1007/s11661-999-0272-9>.
- [18] Zaddach AJ, Niu C, Koch CC, Irving DL. Mechanical properties and stacking fault energies of NiFeCrCoMn high-entropy alloy. *J Occup Med* 2013;65:1780–9. <https://doi.org/10.1007/s11837-013-0771-4>.
- [19] Gludovatz B, Hohenwarter A, Catoor D, Chang EH, George EP, Ritchie RO. A fracture-resistant high-entropy alloy for cryogenic applications. *Science* 2014;345:1153–8. <https://doi.org/10.1126/science.1254581>.
- [20] Gludovatz B, Hohenwarter A, Thurston KVS, Bei H, Wu Z, George EP, et al. Exceptional damage-tolerance of a medium-entropy alloy CrCoNi at cryogenic temperatures. *Nat Commun* 2016;7:10602. <https://doi.org/10.1038/ncomms10602>.
- [21] Deng Y, Tasan CC, Pradeep KG, Springer H, Kostka A, Raabe D. Design of a twinning-induced plasticity high entropy alloy. *Acta Mater* 2015;94:124–33. <https://doi.org/10.1016/j.actamat.2015.04.014>.
- [22] Kumar N, Ying Q, Nie X, Mishra RS, Tang Z, Liaw PK, et al. High strain-rate compressive deformation behavior of the Al_{0.1}CrFeCoNi high entropy alloy. *Mater Des* 2015;86:598–602. <https://doi.org/10.1016/j.matdes.2015.07.161>.
- [23] Easterling KE, Porter David A, Sherif Mohamed Y. *Phase transformations in metals and alloys*. CRC Press; 2009.
- [24] Wani IS, Bhattacharjee T, Sheikh S, Clark IT, Park MH, Okawa T, et al. Cold-rolling and recrystallization textures of a nano-lamellar AlCoCrFeNi_{2.1} eutectic high entropy alloy. *Intermetallics* 2017;84:42–51. <https://doi.org/10.1016/j.intermet.2016.12.018>.
- [25] Saha J, Ummethala G, Malladi SRK, Bhattacharjee PP. Severe warm-rolling mediated microstructure and texture of equiatomic CoCrFeMnNi high entropy alloy: a comparison with cold-rolling. *Intermetallics* 2021;129:107029. <https://doi.org/10.1016/j.intermet.2020.107029>.
- [26] Jinhong P, Ye P, Hui Z, Lu Z. Microstructure and properties of AlCrFeCuNi_x (0.6 ≤ x ≤ 1.4) high-entropy alloys. *Mater Sci Eng, A* 2012;534:228–33. <https://doi.org/10.1016/j.msea.2011.11.063>.
- [27] Tsao LC, Chen CS, Chu CP. Age hardening reaction of the Al_{0.3}CrFe_{1.5}MnNi_{0.5} high entropy alloy. *Mater Des* 1980-2015 2012;36:854–8. <https://doi.org/10.1016/j.matdes.2011.04.067>.
- [28] Zhang H, Pan Y, He Y. Effects of annealing on the microstructure and properties of 6FeNiCoCrAlTiSi high-entropy alloy coating prepared by laser cladding. *J Therm Spray Technol* 2011;20:1049–55. <https://doi.org/10.1007/s11666-011-9626-0>.
- [29] Qin Y, Liu J-X, Li F, Wei X, Wu H, Zhang G-J. A high entropy silicide by reactive spark plasma sintering. *J Adv Ceram* 2020;8. <https://doi.org/10.1007/s40145-019-0319-3>.
- [30] Shen Q, Kong X, Chen X. Fabrication of bulk Al-Co-Cr-Fe-Ni high-entropy alloy using combined cable wire arc additive manufacturing (CCW-AAM): microstructure and mechanical properties. *J Mater Sci Technol* 2021;74:136–42. <https://doi.org/10.1016/j.jmst.2020.10.037>.
- [31] Gromov V, Ivanov Y, Kononov S, Osintsev K, Semin A, Rubannikova Y. Modification of high-entropy alloy AlCoCrFeNi by electron beam treatment. *J Mater Res Technol* 2021;13:787–97. <https://doi.org/10.1016/j.jmrt.2021.05.012>.
- [32] Zhang Y, Chen X, Jayalakshmi S, Singh RA, Deev VB, Prusov ES. Factors determining solid solution phase formation and stability in CoCrFeNi_XO₄ (X=Al, Nb, Ta) high entropy alloys fabricated by powder plasma arc additive

- manufacturing. *J Alloys Compd* 2020;157625. <https://doi.org/10.1016/j.jallcom.2020.157625>.
- [33] Attar H, Calin M, Zhang LC, Scudino S, Eckert J. Manufacture by selective laser melting and mechanical behavior of commercially pure titanium. *Mater Sci Eng -Struct Mater Prop Microstruct Process* 2014;593:170–7. <https://doi.org/10.1016/j.msea.2013.11.038>.
- [34] Li M, Gazquez J, Borisevich A, Mishra R, Flores KM. Evaluation of microstructure and mechanical property variations in AlxCoCrFeNi high entropy alloys produced by a high-throughput laser deposition method. *Intermetallics* 2018;95:110–8. <https://doi.org/10.1016/j.intermet.2018.01.021>.
- [35] Laplanche G, Kostka A, Horst OM, Eggeler G, George EP. Microstructure evolution and critical stress for twinning in the CrMnFeCoNi high-entropy alloy. *Acta Mater* 2016;118:152–63. <https://doi.org/10.1016/j.actamat.2016.07.038>.
- [36] Li Z, Zhao S, Ritchie RO, Meyers MA. Mechanical properties of high-entropy alloys with emphasis on face-centered cubic alloys. *Prog Mater Sci* 2019;102:296–345. <https://doi.org/10.1016/j.pmatsci.2018.12.003>.
- [37] Byun TS, Hashimoto N, Farrell K. Temperature dependence of strain hardening and plastic instability behaviors in austenitic stainless steels. *Acta Mater* 2004;52:3889–99. <https://doi.org/10.1016/j.actamat.2004.05.003>.
- [38] Devincze B, Hoc T, Kubin L. Dislocation mean free paths and strain hardening of crystals. *Science* 2008;320:1745–8. <https://doi.org/10.1126/science.1156101>.
- [39] Tian YZ, Bai Y, Zhao LJ, Gao S, Yang HK, Shibata A, et al. A novel ultrafine-grained Fe22Mn0.6C TWIP steel with superior strength and ductility. *Mater Char* 2017;126:74–80. <https://doi.org/10.1016/j.matchar.2016.12.026>.
- [40] Hamdi F, Asgari S. Evaluation of the role of deformation twinning in work hardening behavior of face-centered-cubic polycrystals. *Metall Mater Trans A* 2008;39:294–303. <https://doi.org/10.1007/s11661-007-9356-6>.
- [41] Gutierrez-Urrutia I, Raabe D. Dislocation and twin substructure evolution during strain hardening of an Fe–22wt.% Mn–0.6wt.% C TWIP steel observed by electron channeling contrast imaging. *Acta Mater* 2011;59:6449–62. <https://doi.org/10.1016/j.actamat.2011.07.009>.
- [42] Gutierrez-Urrutia I, Zaefferer S, Raabe D. The effect of grain size and grain orientation on deformation twinning in a Fe–22wt.% Mn–0.6wt.% C TWIP steel. *Mater Sci Eng, A* 2010;527:3552–60. <https://doi.org/10.1016/j.msea.2010.02.041>.
- [43] Shabani A, Toroghinejad MR, Shafyei A, Cavaliere P. Effect of cold-rolling on microstructure, texture and mechanical properties of an equiatomic FeCrCuMnNi high entropy alloy. *Materialia* 2018;1:175–84. <https://doi.org/10.1016/j.mtla.2018.06.004>.
- [44] Gottstein G. Annealing texture development by multiple twinning in f.c.c. crystals. *Acta Metall* 1984;32:1117–38. [https://doi.org/10.1016/0001-6160\(84\)90015-4](https://doi.org/10.1016/0001-6160(84)90015-4).
- [45] Burke JE, Turnbull D. Recrystallization and grain growth. *Prog Met Phys* 1952;3:220–92. [https://doi.org/10.1016/0502-8205\(52\)90009-9](https://doi.org/10.1016/0502-8205(52)90009-9).
- [46] Zhang Y, Shen Q, Chen X, Jayalakshmi S, Singh RA, Kononov S, et al. Strengthening mechanisms in CoCrFeNiX0.4 (Al, Nb, Ta) high entropy alloys fabricated by powder plasma arc additive manufacturing. *Nanomaterials* 2021;11:721. <https://doi.org/10.3390/nano11030721>.
- [47] Haase C, Barrales-Mora LA. Influence of deformation and annealing twinning on the microstructure and texture evolution of face-centered cubic high-entropy alloys. *Acta Mater* 2018;150:88–103. <https://doi.org/10.1016/j.actamat.2018.02.048>.
- [48] Sakai T, Belyakov A, Kaibyshev R, Miura H, Jonas JJ. Dynamic and post-dynamic recrystallization under hot, cold and severe plastic deformation conditions. *Prog Mater Sci* 2014;60:130–207. <https://doi.org/10.1016/j.pmatsci.2013.09.002>.